 FDMP, vol.4, no.1, pp.1-10, 2008

Determination of Non-Equilibrium Surface Tension Gradients in Marangoni Thermal Flows: Application to Aqueous Solutions of Fatty Alcohols

G.Pétré[1], K.Tshinyama, A.Azouni[2], and S. Van Vaerenbergh[1]

Abstract: This study illustrates a relevant and practical method to determine the effective surface tension gradient in a layer subjected to a lateral temperature difference. In general, this can be hardly performed *in situ* without perturbing the flow. For this reason we rely on an indirect determination approach. A simple model is developed that relates the surface tension gradient to other quantities that can be measured without introducing significant disturbances in the system. Measurements of these quantities are performed in a set-up where the flow corresponds with a good approximation to a one-dimensional model. A previously used set-up has been upgraded for such a scope. The observations have been performed in fatty alcohol solutions. The results show that the surface tension gradients responsible for the onset of flow are not equilibrium ones.

Keyword: Marangoni, Surface tension, Non equilibrium.

1 Objectives

Aqueous solutions of fatty alcohols present an equilibrium surface tension minimum as a function of temperature [Vochten, (1973)] in some ranges of temperature and composition. This behaviour is quite peculiar, since for most of fluids, the surface tension decreases when temperature increases, and is thought to induce specific flows in presence of a surface thermal gradient.

A temperature gradient at the interface will create a surface tension gradient inducing a flow that at the interface goes from regions of low surface tension to high surface tension ones (Marangoni effect). Therefore, for aqueous fatty alcohol solutions, one can expect the fluid to flow in the usual manner for surface temperatures below the temperature of the equilibrium surface tension minimum and in the opposed direction when interface temperatures are above the equilibrium surface tension minimum, at least when considering the equilibrium surface tension curve. In the same manner, when the surface temperatures are ranging from below to above the temperature T_m of the minimal surface tension, it can be expected that a thin layer will be "opened", that is to say that for a high enough temperature gradient the solid support of the liquid layer may de-wet. The guessed surface opening of the layer has however never been observed, but experiments performed with aqueous solutions of n-heptanol and n-hexanol showed surface flows from cold to hot regions, even when surface temperatures where below the static surface tension minimum T_m [Pétré, (1993)]. For instance, for water/n-heptanol T_m is at 40°Cbut the Marangoni flow from cold to hot regions has been observed with surface temperatures as low as 8.5 °C[Pétré, (1993)].

These observations show that the equilibrium surface tension curve alone does not allow predicting the flow motion and the surface flow direction in these cases. So far, the actual surface tension gradient remains unknown. The main goal of this work is to determine this quantity.

For this purpose, we carried out experiments on a new set-up allowing temperature measurements and developed a simple theoretical model based on the Navier-Stokes equations.

[1] Université Libre de Bruxelles, Service de Chimie Physique EP, CP 165-62, 50 Av. Roosevelt, 1050 Bruxelles, Belgium

[2] LMSGC, UMR 113 (CNRS-ENPC-LCPC), 2 Allée Kepler 7742A0 Champs sur Marnes, France

2 "One dimensional" process

The purpose of a simple 1-D model is only to describe the flow in a limited region of the experimental device where the observations are performed. (see figure 1). The rectangular coordinates are used to describe the experiment, with x as a horizontal direction, perpendicular to the channels between which positive thermal gradient was created, and with z as a vertical direction . No effect along the third direction was considered, nor was observed in the limits discussed in the next sections.

Both liquid and gas phases are considered viscous and obeying to Boussinesq approximation [Drazin, (1987)]. The density, dynamic viscosity, thermal expansion and heat diffusivity coefficients will be noted respectively ρ, μ, β and χ with "l" subscript for the liquid and "g" for the gas. The stationary flows are governed by the state equations

$$\rho = rho_0 [1 - \beta (T - T_0)] \tag{1}$$

and by the continuity, Navier-Stokes and Fourier equations.

Accounting for Boussinesq approximation and for two-dimensionality, the continuity equation reads

$$\frac{\partial u}{\partial x} = 0 \tag{2}$$

With the same approximations, and after elimination of the pressure, the Navier-Stokes equations are for both phases

$$\frac{\partial^3 u}{\partial z^3} = \frac{\rho_0 . g . \beta}{\mu} \frac{\partial T}{\partial x} \tag{3}$$

and the heat equations

$$\chi \frac{\partial^2 T}{\partial z^2} = u(z) . \frac{\partial T}{\partial x} \tag{4}$$

Taking the derivative of Eq. (3) with respect to x, shows with Eq. (2), that the second derivative of the temperature with respect to x vanishes. Then deriving Eq. (4) with respect to x, shows with Eq. (2) that:

$$\frac{\partial T}{\partial x} = C_1 z + C_2 \tag{5}$$

Using this form of the thermal gradient in the Navier-Stokes Eq. (3) leads to the general form the velocity fields

$$u(z) = \frac{\rho_0 g \beta}{\mu} \left(\frac{1}{24} C_1 z^4 + \frac{1}{6} C_2 z^3 \right) + \frac{1}{2} C_3 z^2 + C_4 z + C_5 \tag{6}$$

When using these analytical forms of the temperature gradient and velocity fields in the two dimensional stationary Fourier Eq. (4), the analytical expressions of the temperature fields are

$$\begin{aligned} T(x,z) = {} & \frac{\rho_0 g \beta}{\mu \chi} \left(\frac{C_1^2}{6.7.24} z^7 + \frac{C_1 C_2}{6.24} z^6 \right) \\ & + \left(\frac{\rho_0 g \beta C_2^2}{5.24 \chi} + \frac{C_1 C_3}{5.8 \chi} \right) z^5 + \left(\frac{C_1 C_4}{3.4 \chi} + \frac{C_2 C_3}{4.6 \chi} \right) z^4 \\ & + \left(\frac{C_1 C_5}{2.3 \chi} + \frac{C_2 C_4}{2.3 \chi} \right) z^3 + \frac{C_2 C_5}{2} z^2 + \Gamma(x) . z + \Gamma^{\circ}(x) \end{aligned} \tag{7}$$

The coefficients C_i (i = 1 to 5) and the functions of z introduced are to be determined from the boundary conditions. It has to be noticed that the temperature profiles of Eq. (7) are more general than those obtained in [Birikh, (1966);Villers, (1987); Kirdyanshkin, (1984)] , since here the horizontal thermal gradient may vary with z, so leading in the velocity fields to the z^4 terms and in the temperature fields to the z^7 terms.

It can be estimated that the deformation of layer thickness by the flow remains inferior to 1% in our experiments. The boundary conditions are therefore taken at a constant height.

The boundary conditions used at the gas/solid and at the liquid/solid interfaces are no slip and constant lateral (horizontal) heat flow:

$$u_g(H) = 0 \qquad u_l(0) = 0 \tag{8}$$

$$\left(\frac{\partial T}{\partial x} \right)_{z=H} = C \quad \left(\frac{\partial T}{\partial x} \right)_{z=0} = A \tag{9}$$

where the C and A are independent of x.

At the liquid/gas interface, a constant lateral heat flux and the velocity continuity are considered, so that

$$u_l(h) = u_g(h) = u_S \tag{10}$$

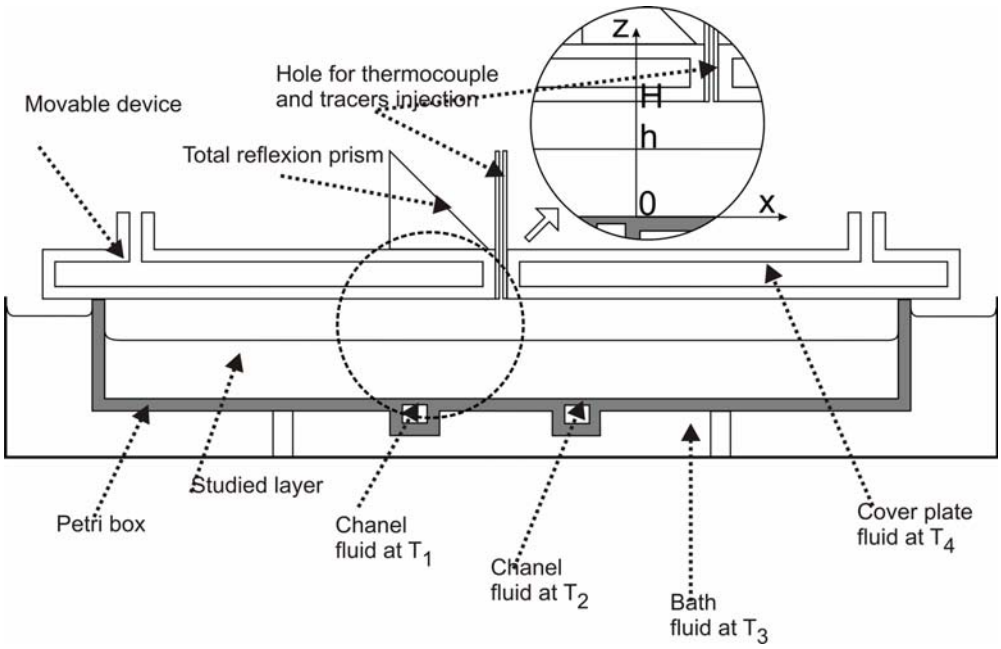

Figure 1: Sketch of the experimental set-up, main dimensions and coordinate system

$$\left(\frac{\partial T}{\partial x}\right)_{z=h} = B \tag{11}$$

where B is independent of x.

From another side, the stress balance at the liquid/gas interface reads

$$\frac{\partial \sigma}{\partial x} = \mu_l \left(\frac{\partial u_l}{\partial z}\right)_{z=h} - \mu_g \left(\frac{\partial u_g}{\partial z}\right)_{z=h} \tag{12}$$

The thermal boundary conditions result from the approximations leading to the expression Eq. (5) of the thermal gradient, and from the assumption that the liquid/gas interface is at constant height h. Other relations determining the unknowns are the conditions

$$\int_0^h u(z).dz = 0 = \int_h^H u_g(z).dz \tag{13}$$

These relations express that the net volumetric flow in each section of the liquid or of the gas layers vanishes and are valid since the set-up is a closed system and as there is no significant mass transfer between phases.

With these conditions for the liquid, one obtains for the velocity profile in the liquid

$$u_l(z) = G_l \left\{ \frac{B-A}{24h} z^4 + \frac{A}{6} z^3 - \frac{3B+7A}{40} h z^2 + \frac{2B+3A}{60} h^2 z \right\} + u_S \left(\frac{3}{h^2} z^2 - \frac{2}{h} z \right) \tag{14}$$

where

$$G_l = \frac{\rho_{0l} g \beta_l}{\mu_l} \tag{15}$$

The conditions for the gas are given by the expression

$$u_l(z) = G_l \left[\frac{B-A}{24h} z^4 + \frac{A}{6} z^3 - \frac{9B+16A}{80} h z^2 + \frac{7B+8A}{120} h^2 z \right] + \frac{1}{4\mu_l h} \left[\frac{\partial \sigma}{\partial x} + \mu_g \left(\frac{\partial u_g}{\partial z} \right)_{z=h} \right] (3z^2 - 2hz) \tag{16}$$

The comparison of the velocity fields' expression allows determining the interface velocity. It is

$$u_S = -\frac{3B+2A}{240} G_l h^3 + \frac{h}{4\mu_l} \left[\frac{\partial \sigma}{\partial x} + \mu_g \left(\frac{\partial u_g}{\partial z} \right)_{z=h} \right] \tag{17}$$

As a by product, one obtains similarly the velocity profile in the gas phase, where appears the parameter

$$G_g = \frac{\rho_{0g} g \beta_g}{\mu_g} \tag{18}$$

With these expressions, one obtains the expression of the interface velocity as a function of measurable temperature gradients and of surface tension gradients

$$\begin{aligned} \frac{\partial \sigma}{\partial x} =& u_S \left(\frac{4\mu_g}{H-h} + \frac{4\mu_l}{h} \right) \\ & - \frac{\rho_{0g} g \beta_g}{60} (H-h)^2 (2C+3B) \\ & + \frac{\rho_{0l} g \beta_l}{60} h^2 (3B+2A) \end{aligned} \tag{19}$$

Recall that the quantities A, B and C are the horizontal temperature gradients at respectively the solid/liquid, the liquid/gas and the gas/solid interfaces. Therefore, the previous relation is between the surface tension gradient and these quantities, for given physico-chemical properties of the liquid and given thickness of the liquid and of the gas layers.

Before presenting the experimental results and using the new expressions of the fields, it is worthwhile to discuss them with respect to the other approximations used in literature.

The unidirectional flow in a horizontal layer submitted to a horizontal temperature gradient assumed constant was considered by several authors [Birikh, (1966);Villers, (1987); Kirdyanshkin, (1984); Villers,(1985)]. These authors assume also that the thermal gradient is constant in the vertical direction. Our results do not use this assumption and are therefore generalizing the results of the above mentioned authors. In particular, the natural convection arising in the gas phase is here quantified (two sided model) and accounted for in the interpretation of the results (see next sections). From another side, some authors have studied the stability of such flows with one sided model [Mercier, (1996); Smith (1983)]. This aspect is not considered here, but we instead focus on experimental conditions where such instabilities should not occur by selecting performing experiments with thin enough layers.

The results obtained here have the advantage of being valid whatever the surface tension dependence on temperature is. It appears here that the velocity profile in the liquid is a linear superposition of three, rather than two, contributions. To the contributions due to buoyancy in the liquid and the one due to surface tension variations, there is a contribution linked to the buoyancy in the gas. Since in practical experiments it is not possible usually to avoid the latter, it should be taken into account in order to accurately link the measurable quantities to the observed flow or to the actual surface tension gradient and/or to design the set up. Obviously, the relative importance of these contributions to the amplitude of the surface velocity depends strongly on the thickness. It can be anticipated that a small thickness of the layer will damp the importance of the buoyancy contributions up to negligible values.

However, the main result is that within the approximations performed, the velocity and the temperature profiles are fully determined by the knowledge of the surface velocity and the horizontal thermal gradients at the three interfaces. Our experimental objective is to measure these quantities that allow evaluating the actual surface tension gradient.

3 Experimental approach

The experimental set-up is adapted from the one used in [Pétré, (1993)]. It has been modified to allow for temperature measurements and video recording of tracers at the liquid surface. The liquid whose surface velocity is to be measured is placed in a PYREX Petri box (of inner diameter of 180 mm, see figure 1). On the underside of the Petri box two parallel glass channels are glued; they aim to create the horizontal thermal gradient in the fluid layers. The distance between the glued glass channels was of 9.8 mm in [Pétré, (1993)] and of 12 mm in this work.

A double-wall glass lid of greater diameter covers the Petri box, to fix the upper temperature at a fixed value, independent of the horizontal position. This temperature is the highest temperature in the set-up, so as to avoid any condensation that could hinder the observations of the liquid/gas in-

terface motions. There are four independent thermostatized baths and the temperatures are set to T_1 for one glass channel, T_2 for the other one, T_3 for the water bath in which the Petri box is immersed, and T_4 for the cover (slid), with $T_1 < T_2 < T_3 < T_4$. This means that the Petri box is placed in a water bath whose temperature is intermediary between the glass channels temperatures.

A small glass tube through the lid allows the introduction of a thermocouple. A thermocouple type K of 0.25 mm diameter was used and its vertical displacement was ensured and measured by a micrometric screw. The lid and the thermocouple were fixed into the frame of the set-up. The lower part of the set-up (that includes the Petri box) was put on a movable plate carried horizontally by a micrometer, so that precise positioning in both horizontal and vertical position of the movable thermocouple can be performed. The temperature measurements are performed once the steady state is reached, and the experiments repeated to ensure reproducibility. The temperatures were so measured at the interfaces and in the bulk liquid and gas phases, so providing among others the temperature gradients A and B.

Measurements of interface velocity are preformed separately. Visualisation of the interface is performed by poring dry talk particles from the above mentioned lid, once the thermocouple is retrieved. Velocimetry is performed once the steady state is reached, by video records of the interface image obtained with a profile projector (magnifying by 10 on the screen) and the velocities deduced by measuring the time needed to travel over given distances on the free surface (3 and 5 mm). The tracers (talc) velocity at the surface was monitored with a CCD camera through a total reflection prism (see figure 1).

The liquid thickness is 1.8 mm (50 ml of liquid). The gas layer thickness is 18 mm. The set up is such that the flow is irrotational in the observed zone. No hydrodynamic instability are likely to occur (nor were observed) in the liquid with the experimental configuration and the range of parameters selected for our experiments, consistently with the stability analysis performed by [Villers,(1985); Mercier, (1996); Smith ,(1983)].

The systems studied here are pure water and a 6.18 mili-molal aqueous solutions of n-heptanol. Note that the water/n-heptanol solution has minimum value of the equilibrium surface tension located at a temperature close to 40°C[Vochten,(1973)].

Experiment were first performed in pure water to calibrate the system, and then in the water/n-heptanol solution. The main experimental conditions used are reported in table 1.

4 Results of experiments in water

With the experiments performed in pure tridistliled water, we wished to validate the proposed analytical model linking surface velocities to surface tension gradients and thermal gradients (Equation (19)). The usual delicate precautions and procedure to avoid surface contamination were used. The imposed temperatures are given in table 1. We approximate the values of the physico-chemical coefficients of the liquid and gas phases by respectively these of water and moist air at the average temperature of the surface (28°C) and at 1 atm.

$$\rho_{0l} = 996 kg/m^3, \quad \rho_{0g} = 1.17 kg/m^3$$

$$\beta_{0l} = 0.28510^{-3} K^{-1}, \quad \beta_{0g} = 3.310^{-3} K^{-1}$$

$$\mu_l = 0.83310^{-3} N/m^2, \quad \mu_g = 1.8710^{-5} N/m^2$$

The gradients A and B are respectively deduced from these measurements of the temperatures recorded in the liquid at the bottom rigid wall and at the liquid/gas interface millimetre by millimetre. For imposed temperature gradients above 1400 K/m, the tracer trajectories started being 2-D and remained 2-D in a lateral extension larger than the distance between the channels. Ulterior experiments were performed below this gradient, and could verify in addition of the one dimensionality of the flow, a good uniformity in the region between the channels. As an example, when $T_2 - T_1$ = 6.9 K, the video records provide a mean velocity of surface tracers of - 4.48 mm/s (from hot to cold regions) on a span of 3 mm, and a velocity of - 4.50 mm/s on a span of 5 mm. The mean value of - 4.49 mm/s is considered as usable for the model.

Table 1: Main experimental conditions

system	T_1 (K)	Range of T_2 (K)	T_3 (K)	T_4 (K)
Water	303	307 to 313	303.4	315
Water/n-heptanol 6.18 10^3 moles/kg	298.4	303.6 to 310	301.6	315

Table 2a summarizes the main overall experimental results for pure water.

The last column provides the mean values of the surface velocities for different values of the thermal gradient. From these and using the relation (19), we deduce the corresponding surface tension gradient (first column of table 2b). This quantity is referred here as the "measured surface tension gradient".

Table 2b also provides the ratio of the measured surface tension gradient by the measured free surface thermal gradient (column 3). This ratio fits well the variation with temperature of the equilibrium surface tension (fourth column) i.e (-0,0004 T - 0,1448) mN/(m K) where T is in °C. This provides good confidence that our model is usable for the measurement of the surface tension gradient.

5 Results of experiments in water/n-heptanol

The results obtained in water/n-heptanol are now detailed. The particles moved always from the cold region to the hot one, although the surface temperatures were below the temperature of the minimum of equilibrium surface tension. These observations were reproduced up to a surface temperature of 8.5 °C. The surface velocities at the temperature of the surface tension minimum, instead of vanishing, were of the order of 3 10^{-4} m/s for a difference of temperature between the channels of $T_2 - T_1 = 6$ K.

Table 3a summarises the results of surface tension measurements in the heptanol aqueous solution. The values are the average values of experimental points considered as statistical series: temperatures as function of position, velocity as function of position. The "error cross bars" presented in table 3a and figures 2 and 3 correspond to twice the standard deviation ("two sigma") for the temperature gradients, and to half the standard deviation for the velocities.

As compared to pure water, but for the same temperature difference between the solids walls and a same temperature difference between the channels, the velocities are a few times smaller than in water and of opposed sign, that is to say, from cold to hot. Measured liquid temperature gradient at the solid interface (A) is a few times larger than in water. Typical shapes of gradients are shown in fig. 2.

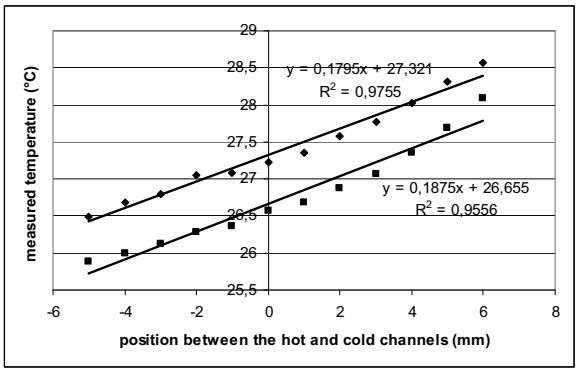

Figure 2: Example of measurements of liquid temperatures in water n-heptanol solutions at the liquid/solid and the liquid/gas interface

The relation between gradients B and A is shown in (Figure 3). The dependence does not seem perfectly a linear one and, although it is not obvious to decide of this question within the experimental uncertainties, a better correlation seems more quadratic for high gradients. The surface velocity is displayed in figure 4 versus the applied gradient (gradient A) and in figure 5 versus the liquid/gas interface measured temperature (gradient B).

The surface velocity does not depend linearly on any of these gradients and the best polynomial fit is a quadratic one. In the third column of table 3b appears the "measured surface tension gradient"

Table 2a: Measurements performed in water (see also table 1). Set temperature differences and measured gradients at the solid interface (A), at liquid gas interface (B), surface velocities measured on a span of 3 and 5 mm, and the mean value considered.

Applied $(T_2 - T_1)$ (K)	Measured Liq/sol gradient A (K/m)	Mean interface temp. (K)	Measured Liq/gas gradient B (K/m)	Measured mean surface velocity u (10^{-2}m/s)		
				on 3 mm.	on 5 mm	Mean value
4	53.3	305	28.6	-2.61	-2.62	-2.61
6.9	89.9	306.45	49.9	-4.48	-4.50	-4.49
8.5	111	307.25	59.9	-5.44	-5.78	-5.61
10	142	308	75	-6.79	-6.82	-6.81

Table 2b: Analysis of experiments in water: value of the surface tension gradient deduced from table 2 with expression (19), mean surface temperature, experimental surface tension/temperature coefficient, and equilibrium value of the surface tension / temperature coefficient

$\frac{\partial\sigma}{\partial x}$ (10^{-5}N/m^2)	Mean interface temperature (K)	$\frac{\partial\sigma}{\partial x}$/B ($10^{-5}$N/m/K)	$\left(\frac{\partial\sigma}{\partial T}\right)_{eq}$ (10^{-5}N/m/K)
-45.9	305	-1.60	-1.576
-79.2	306.5	-1.59	-1.587
-92.8	307	-1.55	-1.587
-119	308	-1.59	-1.588

Table 3a: Analysis of experiments in a water-heptanol solution: driving set temperature difference between the channels (T_2-T_1), measured mean temperature gradient at the interface (B), the surface tension gradient deduced from table 3 with expression (19), and the product of the equilibrium surface tension coefficient by B.

Applied $(T_2 - T_1)$ (K)	Measured Liq/sol gradient A (K/m)		Mean interface temp. (K)	Measured Liq/gas gradient B (K/m)		Measured mean surface velocity u (10^{-3}m/s)	
	A	3σ		B	$3\,\sigma$	u	$1/2\sigma$
3.37	180	12	299.95	187	7	0.27	0.049
5.31	251	28	300.85	312	17	0.31	0.057
5.61	315	68	300.55	461	19	0.43	0.062
7.35	440	29	301.85	564	29	0.72	0.236
8.67	514	37	301.45	331	22	0.67	0.187
11.12	512	69	300.65	440	102	1.14	0.063
11.43	596	60	302.65	467	17	1.46	0.339
12.24	696	74	302.55	547	58		
12.96	753	3	302.55	597	3	1.62	0.394

Table 3b: Analysis of measurements performed in a water-heptanol solution (see also table 1): measured surface tension gradient, mean temperature of interface, ratio of surface tension gradient to surface temperature gradient and equilibrium value of the surface tension/temperature coefficient.

$\frac{\partial\sigma}{\partial x}$ (10^{-5}N/m^2)	Mean interface temperature (K)	$\frac{\partial\sigma}{\partial x}$/B ($10^{-5}$N/m/K)	$\left(\frac{\partial\sigma}{\partial T}\right)_{eq}$ (10^{-5} N/m^2/K)
50.6	299.9	2.71	-0.98
58.8	300.8	1.88	-0.89
80.8	300.5	1.75	-0.92
134	301.8	2.38	-0.80
126	301.4	3.81	-0.84
212	300.6	4.82	-0.91
272	302.6	5.82	-0.73
343	302.5	5.75	-0.74

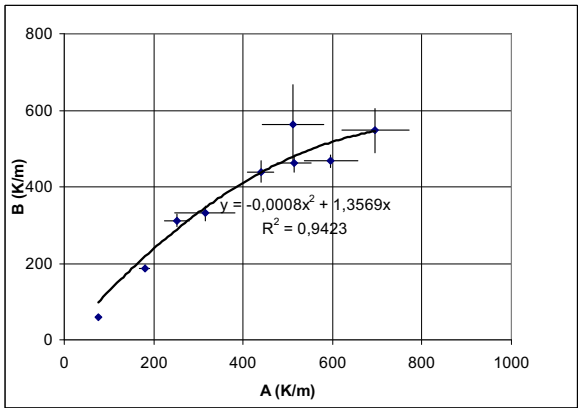

Figure 3: Correlation between the measured mean thermal gradients at the liquid/solid interface (A) and at the liquid/gas interface (B)

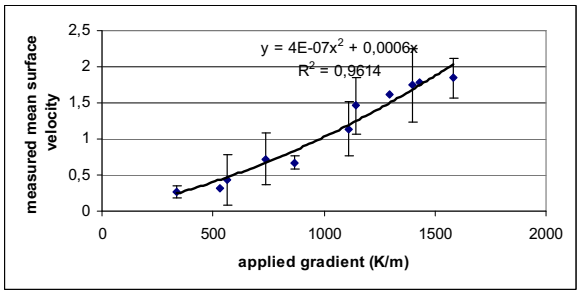

Figure 4: Free surface velocities (u_s) as a function of the gradient applied at the level of the channels. The 3 points without crossbars are the estimates obtained with a single measurement (not reported on tables)

$d\sigma/dx$ deduced as for pure water from formula (19). The static surface tension/temperature coefficient multiplied by the measured free surface thermal gradient is provided in the fourth column of table 3b. The good agreement found above for water, collapses for water-n-heptanol. This disagreement is mainly on the sign, as shown on figure 6.

The flow is going from the hot region to the cold one, although the interface temperature is below the minimal surface tension temperature. Note that in the set-up we used, the terms involving buoyancy are together inferior to 1% to the obtained value of the surface tension gradient. For

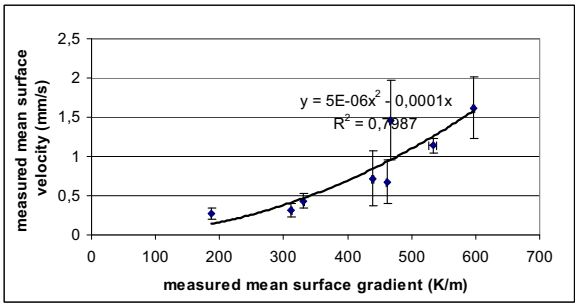

Figure 5: : free surface velocities (u_s) as a function of the measured mean gradient at the liquid/gas interface (B). The correlation is forced to pass by origin

instance, comparing the different thermal contri-

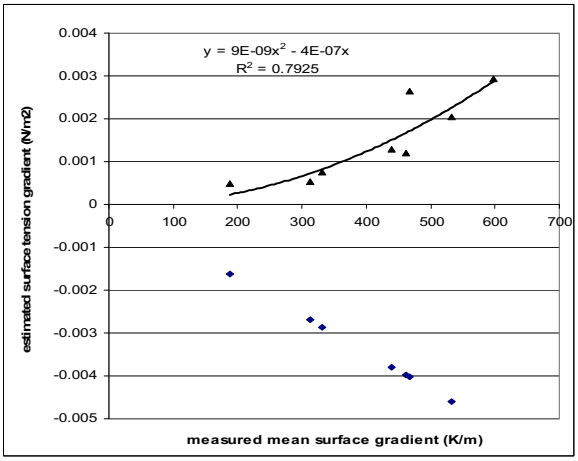

Figure 6: Estimation of the surface tension gradient obtained with formula (19) versus the measured gradients. Triangles refer to the measured velocities and diamond shapes refer to product B by the equilibrium surface tension temperature coefficient

butions in expression (19) in the measurement where B is 187 K/m, the liquid dynamic pressure is 1.38 10^{-5}mN/m, the gas dynamic pressure is – 1.15 mN/m, and the sum of both is 0.23 mN/m, to be compared to computed surface tension gradient of 50.6 mN/m. It can be estimated that an evaporation induced solutal contribution in the buoyancy terms is also negligible thanks to the small thickness chosen for the gaz and liquid layers. This smallness of buoyancy contribution is however not a general case and in particular around 8°C, where we observed that the surface velocity decreases significantly. In any case, although we obtained an experimental measurement of the actual surface tension gradient, it seems interesting to consider later on the influence of additional mechanisms, linked to interface thermal conditions, in order to explain the inversion on the flow sign and the shift of the temperature of the surface tension minimum.

6 Conclusions

In this paper we reported experiments on surface tension driven phenomena in water and in aqueous fatty alcohol solutions and developed a simple theoretical model based on the Navier-Stokes equations in order to determine the effective surface tension gradient at the liquid-gas interface. The experimental set-up was adapted to mimic the theoretical constraints of the model. We succeeded to validate this model in the case of pure water – well documented in literature – and clearly showed that for the heptanol aqueous solution, the experimentally determined surface tension gradient involves other major non-equilibrium processes. Further studies and elaboration are required along these lines.

Acknowledgement: We acknowledge J.-C Legros for support and distinguished advise and comments and the Belgian PRODEX program SIMBA.

References

Atluri, S. N.; Nakagaki, M. (1986): Computational methods for plane problems of fracture. In: S. N. Atluri (ed) *Computational methods in the mechanics of fracture*, Elsevier, Amsterdam, pp. 169-227.

Birikh, R.V. (1966): Thermocapillary convection in horizontal layer of liquid. *J. Appl. Mech.Tech. Phys*.7, 43.

Drazin, P.D.; Reid W.H. (1987): Hydrodynamic stability. *Cambridge University Press*.

Handbook of Chemistry and Physics, (1975-1976): 56^{th} edition, *CRC press*, Cleveland, Ohio

Kirdyanshkin, A.G. (1984): Thermogravitational and Thermocapillary flows in a horizontal liquid layer under the conditions of a horizontal temperature gradient, *Int. J. Heat Transfer*, 27(8), 1205.

Mercier J.F.; Normand C. (1996): Buoynat-thermocapillary instabilityies of differentially heated liquid layers, *Phys. Fluids*, 8 (6), 1433.

Pétré, G.; Azouni, M.A.; Tshinyama, K. (1993): Marangoni Convection at alcohol aqueous solutions-air interfaces., *Appl.Sci.Res*. 5, 97.

Smith, M.K.; Davis, S.H. (1983): Instabilities of dynamic thermocapillary liquid layers. Part I. Convective instabilities, *J. Fluid Mech*., 132, 119.

Villers D.; Platten, J.K. (1985): Marangoni con-

vection in systems presenting a minimum of surface tension, *PhysicoChemical Hydrodynamics*, 5 (4), 435.

Villers, D.; Platten, J.K. (1987): Separation of Marangoni Convection from Gravitational Convection in Earth Experiments, *PhysicoChemical Hydrod*, 173.

Vochten, R.; Pétré, G. (1973): Study of heat of reversible adsorption at the air-solution interface, *European Biophysics Congress, Vienna*, 417-423 or the sames in J. Coll. Interf. Sci. 42, 320.